Int. J. Heat Mass Transfer. Vol. 14, pp. 223–243. Pergamon Press 1971. Printed in Great Britain

LAMINAR HEAT TRANSFER IN THE THERMAL ENTRANCE REGION OF CIRCULAR TUBES AND TWO-DIMENSIONAL RECTANGULAR DUCTS WITH WALL SUCTION AND INJECTION

G. RAITHBY

Department of Mechanical Engineering, University of Waterloo, Waterloo, Ontario, Canada

(*Received* 17 *February* 1970 *and in revised form* 5 *May* 1970)

Abstract—Developed velocity profiles, for flows with mass addition or withdrawal through the boundary, are reported for both circular tube and two-dimensional rectangular duct geometries. For flow in a two-dimensional duct, a new solution was found, which suggests the possibility of a transition to turbulence induced by suction. Equations representing the friction coefficients are presented for both geometries. The development of the temperature field, in a region of fully developed velocity, is analysed for both ducts and for constant temperature and constant heat flux boundary conditions. The nearly universal dependence of the heat transfer results on a single parameter, namely, a Péclét number based on the velocity of the fluid crossing the wall, is demonstrated. Several asymptotic solutions to the energy equation are obtained for high rates of mass addition and withdrawal.

NOMENCLATURE

A_d, constant for duct flow, equation (11);
A_t, constant for tube flow, equation (5);
C_f, wall friction coefficient (wall shear/$\frac{1}{2}\rho u^2$);
C_i, Fourier coefficients, equation (20);
C_p, specific heat at constant pressure;
$f(\zeta)$, similarity variable, equation (3) for tube flow, equation (9) for duct flow;
$F(\eta)$, similarity variable, equations (3A) and (3B);
G_i, eigenfunctions, equation (18);
$h(\zeta)$, see equations (24) and (25);
H, half height of duct, Fig. 1;
j, integer, $j = 0$ for duct flow, $j = 1$ for tube flow;
k, thermal conductivity;
Nu, Nusselt number, $2Rq_W/k(T_B - T_W)$ for tube, $2Hq_w/k(T_B - T_W)$ for duct;
p, pressure;
Pe_W, wall Péclét number, $Re_W Pr$;
Pr, Prandtl number, $\mu C_p/k$;
q_W, wall heat flux;
r, radial coordinate, Fig. 1;
R, tube radius;
Re, Reynolds number, $2R\rho u/\mu$ for tube, $2H\rho u/\mu$ for duct;
Re_W, wall Reynolds number, $\rho v_w 2R/\mu$ for tube, $\rho v_w 2H/\mu$ for duct;
t, time;
T, temperature;
u, axial velocity;
$\bar{u}$, mean axial velocity;
v, velocity normal to wall;
w, weighting function;
x, coordinate parallel to wall, Fig. 1;
y, coordinate normal to duct wall;
β_i^2, eigenvalues, equation (18);
ζ, dimensionless coordinate, y/H for duct, r/R for tube;
η, dimensionless coordinate, $(r/R)^2$;
θ, $(T - T_W)/(T_0 - T_W)$ for C.W.T. bound-

ary condition, $k(T-T_0)/q_W R$ for C.H.F. boundary condition, tube geometry, $k(T-T_0)/q_W H$ for C.H.F. boundary condition, duct geometry;

θ^*, difference temperature, equation (32);

μ, absolute viscosity;

ξ, dimensionless coordinate, x/R for tube, x/H for duct;

ρ, fluid density;

χ, inverse Graetz number, $(x/R)/Re_0 Pr$ for tube, $(x/H)/Re_0 Pr$ for duct.

Subscripts

B, bulk condition;

$\mathfrak{C}$, centerline condition;

fd, thermally developed condition;

j, subscript on $f(\zeta)$, $j=0$ for duct flow, $j=1$ for tube flow;

0, conditions where heating begins, $x=0$;

W, conditions at the wall.

INTRODUCTION

It was demonstrated nearly two decades ago, that the equations of motion for laminar, fully developed flow in circular tubes or two-dimensional rectangular ducts, with fluid injection or withdrawal through the boundaries, could be reduced to a single, fourth order, non-linear, ordinary differential equation. This equation was initially solved using perturbation techniques. Fully numerical solutions were obtained first by Eckert *et al.* [1] and Berman [2]. For the circular tube geometry, both of these investigations revealed a multiplicity of solutions for certain ranges of suction velocity, and established that, at a certain critical suction rate, the velocity gradient at the wall became zero. Berman pointed out that, for the circular tube geometry, suction could therefore induce a transition to turbulence. No corresponding situation has been reported for the two-dimensional rectangular duct geometry. The question of a suction induced transition and a multiplicity of solutions for this geometry is considered here.

Kinney [3] computed friction coefficients for fully developed laminar tube flow and pointed out the importance of these for studies of interfacial stress between a vapour flowing in the core of a tube and the liquid condensate film on the wall. The corresponding calculations for two-dimensional duct flow have not been reported and equations from which the friction coefficients can be directly computed are not available. From the remarkably different influence of suction and injection on the velocity profiles in circular tubes compared to rectangular ducts [2], the friction coefficients would also be expected to display distinctly different characteristics. The present investigation also deals with these questions.

The interaction of wall mass transfer and heat transfer has received little attention. Yuan and Finkelstein [4] carried out a perturbation solution for small injection rates to show the effect of a step change in tube wall temperature. Kinney [3] computed the fully developed temperature profiles for flow in a circular tube at constant wall temperature. The present investigation deals with the problem of thermal development in a region of fully developed velocity in rectangular ducts and circular tubes for both constant wall temperature and constant heat flux boundary conditions. The results (namely, the fully developed temperature profiles and Nusselt numbers as well as development lengths) for each of the four separate cases are shown to depend almost exclusively on a single parameter, a Péclét number based on the suction or injection velocity. In addition, comparisons are made to show the influence of the duct geometry and the thermal boundary condition on the heat transfer results. Independent of, and simultaneous to, the present investigation Pederson [9] solved one of these cases, namely the problem of thermal development in a circular tube at constant wall temperature. The form of Pederson's solution is different than that presented here.

It should be noted that solutions of the thermal development problem are directly applicable to problems involving the flow of a binary gas where one component of the gas is evaporating

or condensing at the wall. If the Schmidt number replaces the Prandtl number, then the concentration profile of the condensing or evaporating component will be the same as the temperature profile (provided the boundary conditions are the same) and the Nusselt number for diffusive mass transfer corresponds to the Nusselt number for heat transfer [13].

FULLY DEVELOPED VELOCITY PROFILE ANALYSIS

Several investigators have computed the fully developed velocity profiles in circular tubes (referred to here as tubes) and two-dimensional rectangular channels (ducts) with suction and blowing through the wall. Berman [2] provides an excellent review. The discussion here will briefly describe some new developments in this problem. A short review will provide the necessary background.

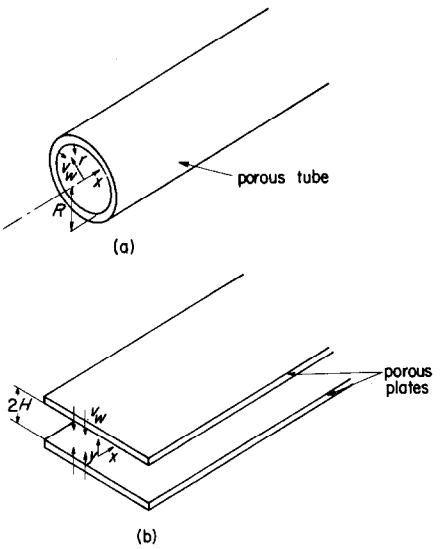

FIG. 1. Geometries and coordinate systems.

It is assumed that the flow through the tube and duct is two-dimensional, symmetric, steady, laminar, and has no significant property value variations. The rate of mass transfer through the wall is also assumed uniform. The usual coordinate systems are shown in Fig. 1.

The appropriate momentum and continuity equations are conveniently written in vector notation as

$$\frac{DV}{Dt} = -\frac{1}{\rho}\nabla P + \frac{\mu}{\rho}\nabla^2 V, \text{ where } \frac{\partial V}{\partial t} = 0 \tag{1}$$

$$\nabla . V = 0. \tag{2}$$

∇^2, the Lapacian, has the form appropriate to the coordinate system (rectangular for the duct, cylindrical for the tube). V is the two-dimensional velocity vector with components u and v respectively in the x and r (tube) or y (duct) directions.

Tube flow. Yuan and Finkelstein [5] proposed that, in the fully developed region, $u/\bar{u}$ should be a function only of $\eta = (r/R)^2$.
For example

$$u = 2\bar{u}F'(\eta) = \bar{u}\frac{f_1'(\zeta)}{\zeta}. \tag{3A}$$

To satisfy the continuity equation

$$v = -2v_W F(\eta)/(\sqrt{\eta}) = -2v_W \frac{f_1(\zeta)}{\zeta}. \tag{3B}$$

The expressions for u and v in terms of functions of ζ will be used in a later section. Substituting u and v into equation (1), it can be shown [2, 3] that F is described by the differential equation

$$\eta F''' + F'' - \frac{Re_W}{2}(F'^2 - FF'') + \frac{A_t}{16} = 0 \tag{4}$$

$$\text{where } A_t = -\frac{Re}{\rho\bar{u}^2}\frac{\partial P}{\partial \xi}$$

$$= -\frac{Re_0}{\rho\bar{u}_0^2}\frac{1}{[1 + 2\xi(Re_W/Re_0)]}\frac{\partial P}{\partial \xi}. \tag{5}$$

Four boundary conditions are required to determine F and A_t in equation (4).
These are

at $r = R$ or $\eta = 1$
(a) $v = -v_W$ or $F(1) = \frac{1}{2}$
(b) $u = 0$ or $F'(1) = 0$

$$\text{at } r = 0 \text{ or } \eta = 0$$
$$\text{(c) } v = 0 \qquad \text{or } F(0) = 0$$
$$\text{(d) } \frac{\partial u}{\partial r} = 0 \qquad \text{or } \lim_{\eta \to 0}(\sqrt{\eta})F''(0) = 0. \tag{6}$$

Boundary condition (d), equation 6, is difficult to handle numerically since no definite value is assigned to $F''(0)$. Berman [2] avoided this problem by writing equation 4 in terms of ζ but in this case one must solve an integro-differential equation. Eckert *et al.* [1] integrated from $\eta = 1$ to $\eta = 0$ and used, instead of condition (d), the relation $\eta F'''(0) = 0$; difficulties were encountered evaluating $F'''(0)$. In the present investigation, condition (d) was replaced by the constraint

$$F''(0) = \frac{Re_W}{2}[F'(0)]^2 - \frac{A_t}{16}. \tag{7}$$

Since $F'(\eta)$ represents the velocity ratio $u/2\bar{u}$, $[F'(0)]^2$ must remain finite and $F''(\eta)$ and $F'(\eta)$ must be continuous. It follows therefore, that equation 7 guarantees that $\lim_{\eta \to 0}(\sqrt{\eta})F''(0) = 0$. If, in addition, $F'''(\eta)$ is finite and continuous, the two conditions can be shown to be exactly equivalent.

In a numerical integration scheme, a starting value of $F'''(0)$ is required. From equations (4) and (7) it follows that

$$F'''(0) = \frac{Re_W}{4} F'(0)\, F''(0).$$

After replacing condition (d), equation (6), by equation (7) and by utilizing the above equation for $F'''(0)$, equation (4) was numerically integrated to obtain values of A_t and distributions of F, F' and F'' to an accuracy of about 9 significant figures.

The results of the velocity profile computations are well summarized by Berman [2]. It seems appropriate to give a brief review so that a comparison can be made with some new developments for the duct flow case.

For no wall mass transfer ($Re_W = 0$), equation (4) yields the usual parabolic velocity profile, $u/\bar{u} = 2(1 - \eta)$ (Fig. 2A). The axial pressure gradient, related to A_t in equation (4) by equation (5), is negative ($A_t = +16$). For mass injection ($Re_W > 0$), the velocity profile ($u/\bar{u}$),

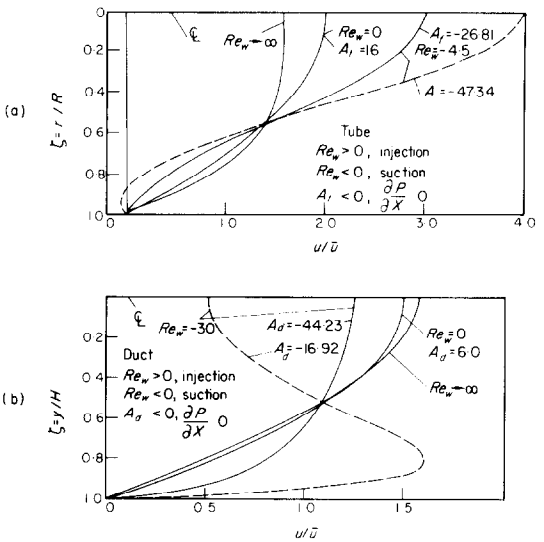

FIG. 2. Fully developed velocity profiles for tubes (a) and two-dimensional ducts (b).

becomes gradually fuller; Yuan and Finkelstein [5] have shown that $u/\bar{u} = 2F'(\eta) \to \pi/2 \cos \pi\eta/2$ for large Re_W. The pressure gradient remains negative as indicated by a monotonically increasing value of A_t with Re_W. For large Re_W, $A_t \to 2\pi^2[1 + (Re_W/4)]$. Kinney [3] has shown that the friction coefficient, C_f, increases with Re_W for a given local Reynolds number, Re. From the above velocity profile for asymptotically large Re_W, $C_f \to 2\pi^2/Re$. The dependence of $C_f Re$ on Re_W is shown in Fig. 3. The following empirical equation accurately represents the data for negative as well as positive Re_W:

$$C_f Re = \left(0{\cdot}0481 + \frac{0{\cdot}0494}{(Re_W + 4{\cdot}70)^{0{\cdot}800}}\right)^{-1}. \tag{8}$$

With increasing wall suction ($Re_W < 0$), the pressure gradient increases to zero and becomes positive for large enough suction. This perhaps surprising fact can be understood by writing a momentum balance over the cross-section of

the tube. The velocity gradient at the wall, and therefore C_f also, decreases and becomes zero, according to the present calculations, for $-4{\cdot}5980 < Re_W < -4{\cdot}5978$; this value agrees closely with Berman's calculations but is considerably different than the value given by Kinney [3]. If other solutions to equation (4) are sought for smaller suction rates ($Re_W > -4{\cdot}5978$), a second is found [1, 2] in which $u/\bar{u}$ becomes negative near the wall, i.e. backflow

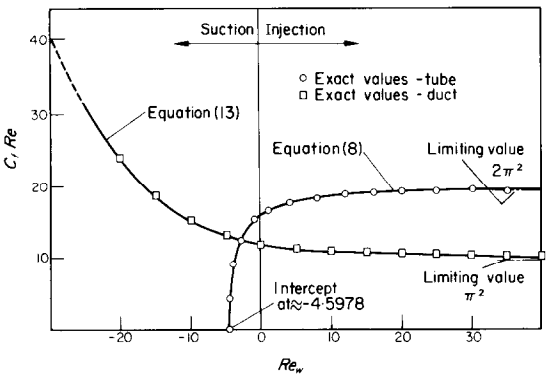

FIG. 3. "Exact" friction coefficients and empirical equations for the region of fully developed flow.

occurs. The solutions become identical as Re_W decreases and approaches the critical value ($Re_W \approx -4{\cdot}5978$); the two solutions are shown in Fig. 2A for $Re_W = -4{\cdot}5$. Thwaites [6] has also shown the possibility of two flows, one with backflow, in a two-dimensional diffuser with wall suction. It appears unlikely, in the tube flow case, that the second profile would ever be physically realized since the accompanying adverse pressure gradient is very large compared to that for the first solution (see A_t values in Fig. 2).

In the presence of the adverse pressure gradient, the profile with backflow, if it could be produced, would probably become quickly turbulent. The profile that seems physically possible also takes on a less stable shape, and must flow against an increasingly adverse pressure gradient, as the suction is increased. As Berman [2] points out, suction could induce a transition to turbulence for values of Re at which a flow would be normally stable. For external flows, where the pressure gradient is not dependent on the suction rate, suction actually increases, rather than decreases, the flow stability.

Two-dimensional duct flow. In the fully developed region, Berman [7] suggested that $u/\bar{u}$ be a function of $\zeta = y/H$ alone. In this investigation, the relationship used was

$$u = 2\bar{u} f_0'(\zeta). \tag{9A}$$

To satisfy the continuity constraint, equation (2),

$$v = -2v_W f_0(\zeta). \tag{9B}$$

The momentum equation, equation (1), is satisfied if f_0 is the solution to

$$f_0''' + Re_W[f_0 f_0'' - (f_0')^2] + \frac{A_d}{4} = 0 \tag{10}$$

where

$$A_d = -\frac{Re}{\rho\bar{u}^2}\frac{\partial P}{\partial \xi} = -\frac{Re_0}{\rho\bar{u}_0^2} \times \left[\frac{1}{[1 + \xi(Re_W/Re_0)]}\right]\frac{\partial P}{\partial \xi}. \tag{11}$$

A_d is a function of Re_W alone. The four boundary conditions necessary to determine f_0 and A_d from equation (10) are

$$\left.\begin{aligned} &\text{at } y = H \text{ or } \zeta = 1 \\ &\qquad \text{(a) } v = -v_W \text{ or } f_0(1) = \tfrac{1}{2} \\ &\qquad \text{(b) } u = 0 \quad \text{or } f_0'(1) = 0 \\ &\text{at } y = 0 \text{ or } \zeta = 0 \\ &\qquad \text{(c) } v = 0, \quad \text{or } f_0(0) = 0 \\ &\qquad \text{(d) } \frac{\partial u}{\partial y} = 0 \quad \text{or } f_0''(0) = 0. \end{aligned}\right\} \tag{12}$$

For no wall mass transfer ($Re_W = 0$), equations (10) and (12) yield the usual parabolic profile, $u/\bar{u} = 3/2\,(1 - \zeta^2)$, and a negative axial pressure gradient (in equation (11), $A_d = 6{\cdot}0$). With increasing blowing, the $u/\bar{u}$ profile becomes only very slightly less full; as $Re_W \to \infty$ Yuan [8] has shown that $u/\bar{u} \to \pi/2 \cos(\pi\zeta/2)$. The profiles for $Re_W = 0$ and $Re_w \to \infty$ are shown in

Fig. 2B. As Re_W increases, the axial pressure gradient also becomes more favourable, as reflected in the monotonically decreasing value of $-A_d$ shown in Fig. 4 (solid line).

As opposed to the tube flow case, where a second solution to the momentum equation was found over a certain range of suction, only one solution for duct flow has been reported. The suction profile for $Re_W = -30$ is indicated in Fig. 2B by the solid line. As $Re_W \to -\infty$, the velocity profile has been shown to become progressively flatter so that $u \to \bar{u}$ everywhere

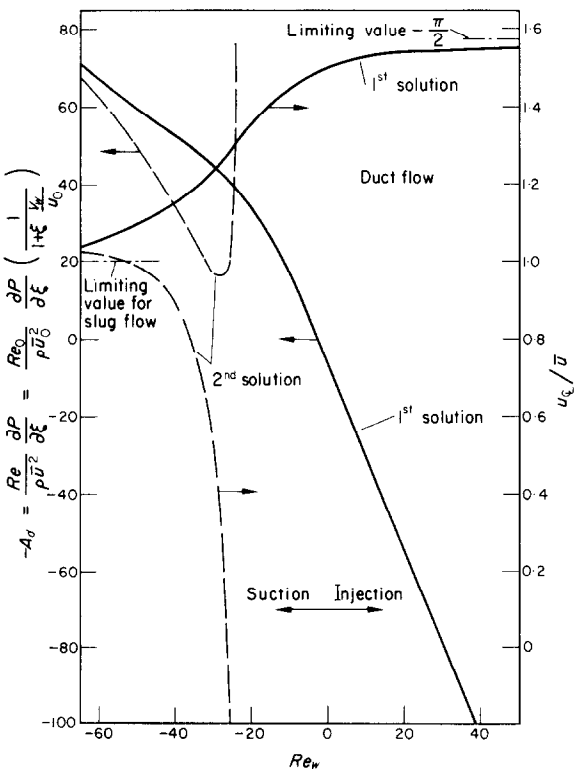

FIG. 4. Dependence of pressure gradient parameter and $\bar{u}/u_{\xi}$ on Re_W for the two possible solutions for fully developed duct flow.

in the duct. The fullness of the profile is reflected in the ratio of the centreline velocity to the mean velocity, $u_{\xi}/\bar{u}$. The change in this ratio with Re_W, and the asymptotic limits for $Re_W \to \infty$ and $Re_W \to -\infty$, are shown in Fig. 4 by the solid line.

As the suction increases and the profile becomes flatter, the gradient at the wall, and therefore C_f, must increase. By an analysis similar to Kinney's [3], it is possible to show that, for duct flow also, $C_f Re$ is a function of Re_W alone. Values of C_f can be computed from the empirical equation

$$C_f Re = \pi^2 + \exp\left[\sum_{i=1}^{5} a_i (Re_W)^{i-1}\right] \qquad (13)$$

This equation, with $a_1 = 0{\cdot}7757$, $a_2 = -0{\cdot}8149 \times 10^{-1}$, $a_3 = 0{\cdot}1022 \times 10^{-2}$, $a_4 = 0{\cdot}1413 \times 10^{-4}$ and $a_5 = -0{\cdot}4062 \times 10^{-6}$, is compared to the "exact" values in Fig. 3.

With increasing suction, the opposing pressure gradient has been found to become larger, as indicated in Fig. 4 by the increasing value of $-A_d$ (solid line).

From the literature it would appear that the suction-induced instability and the existence of multiple solutions for tube flow have no counterpart in duct flow. However, in a search for additional solutions to equation (10), satisfying all the boundary conditions of equation (12), an additional solution was found for values of Re_W smaller than about -24. The $u/\bar{u}$ profile from this solution for $Re_W = -30$ is shown in Fig. 2B by a broken line. For Re_W values between about -24 and -54, $u/\bar{u}$ has a minimum at the centreline and passes through a maximum before going to zero at the wall; for larger suction rates, $u/\bar{u}$ has a maximum at the centreline and passes through a minimum and another maximum before going to zero at the wall. For very large suction, it appears that this second solution approaches the slug flow profile ($u/\bar{u} = 1$) discussed previously. The ratio of the centreline velocity to the mean velocity, $u_{\xi}/\bar{u}$, is shown for this solution be a broken line in Fig. 4. Note that $u/\bar{u}$ becomes negative, i.e. back flow occurs, in the center of the duct, for values of Re_W close to -24.

In the tube flow case, the second solution had

associated with it a very high opposing pressure gradient. It seems unlikely that such a configuration would be naturally selected by the flow. For duct flow with suction, however, the second solution has associated with it a lower opposing pressure gradient for values of Re_W smaller than about $-24{\cdot}5$. If one gradually increased the suction from zero, the laminar velocity field would apparently correspond to that predicted by the first solution up at least $Re_W = -24{\cdot}5$. Near this suction rate, there is a second velocity profile possible that would result in a lower opposing pressure gradient. Which velocity profile is selected by the flow for higher suction could depend on the inlet velocity profile. If the flow develops towards the second solution, there would likely be a transition to turbulence due to a combination of the velocity profile inflections and the opposing pressure gradient. Re_W, instead of Re, would then be the important parameter in determining flow stability. In any case, an experimental or further analytical investigation would prove interesting.

THERMAL ENTRANCE REGION ANALYSIS

Sufficiently far downstream from the entrance of the tube or duct, the velocity field would become fully developed. The wall and fluid are assumed to have a uniform temperature up to some point, designated by $x = 0$, located in the fully developed region. For $x > 0$ a developing temperature field is considered for two cases: (a) the wall temperature, T_W, is constant and different from the T_W for $x < 0$ (designated C.W.T. case) and (b) the heat flux from the wall, q_W, is constant (designated C.H.F. case). The analysis in both cases assumes a non-dissipative, constant-property flow in which the longitudinal heat conduction is neglected relative to the radial conduction. The energy equation and the associated boundary conditions for the tube are

$$\left.\begin{aligned} &\rho C_p\left(u\frac{\partial T}{\partial x}+v\frac{\partial T}{\partial r}\right)=\frac{k}{r}\frac{\partial}{\partial r}\left(r\frac{\partial T}{\partial r}\right)\\ &x=0,\ T=T_0;\quad r=0,\ \partial T/\partial r=0\\ &r=R,\begin{cases}T=T_W & \text{C.W.T. case}\\ \partial T/\partial r=-q_W/k & \text{C.H.F. case}\end{cases}\end{aligned}\right\}\ \text{tube (14)}$$

and for the duct are

$$\left.\begin{aligned} &\rho C_p\left(u\frac{\partial T}{\partial x}+v\frac{\partial T}{\partial y}\right)=k\frac{\partial^2 T}{\partial y^2}\\ &x=0,\ T=T_0;\quad y=0,\ \partial T/\partial y=0\\ &y=H,\begin{cases}T=T_W & \text{C.W.T. case}\\ \partial T/\partial y=-q_W/k & \text{C.H.F. case}\end{cases}\end{aligned}\right\}\ \text{duct (15)}$$

The C.W.T. case for the tube and duct are considered first.

C.W.T. solutions for tubes and ducts

The development of the temperature field occurs in a region of fully developed velocity. The functions $F(\eta)$ for the tube [or by the transformation in equation (3), $f_1(\zeta)$] and $f_0(\zeta)$ for the duct, related to the fully developed u and v components, are available from the above solutions. Introducing $f_j(\zeta)$ into equations (14) and (15), where $j = 1$ for tube flow and $j = 0$ for duct flow, changing coordinates to ζ and χ and setting $\theta = (T - T_W)/(T_0 - T_W)$ one obtains

$$\frac{1}{f_j'}\frac{\partial}{\partial\zeta}\left(\zeta^j\frac{\partial\theta}{\partial\zeta}\right)+\frac{f_j}{f_j'}Pe_W\frac{\partial\theta}{\partial\chi}=\frac{1}{(j+1)}\frac{\bar{u}(\chi)}{\bar{u}_0}\frac{\partial\theta}{\partial\chi}. \tag{16}$$

For tube flow $j = 1$, for duct flow $j = 0$.

A Péclét number, defined by $Pe_W = Re_W Pr$ has been introduced; for mass injection, this parameter physically represents the ratio of radial heat convection to radial heat conduction. Its physical meaning for flow with mass withdrawal is examined below.

If the axial conduction term had not been neglected, the term $-(Re_0 Pr)^{-2}\partial^2\theta/\partial\chi^2$ would be added to the right-hand side of equation (16).

For $(Re_0 Pr)^2 \gg 1$, it would appear that this term could be neglected. For flow with suction, where the heating is not begun until most of the mass has been withdrawn, this condition will not be satisfied.

Utilizing a mass balance to express $\bar{u}/\bar{u}_0$ in terms of Pe_W, the solution to equation (16) with associated boundary conditions is found, by the Graetz method, to be

$$\theta = \sum_{i=1}^{\infty} C_i[1 + (1 + j)Pe_W\chi]^{-\beta_i^2/Pe_W} G_i(\zeta). \quad (17)$$

G_i and β_i^2 are respectively eigenfunctions and eigenvalues of the problem

$$\begin{aligned} &\zeta^j G_i'' + (j + f_j Pe_W) G_i' + \beta_i^2 f_j' G_i = 0 \\ \text{b.c.} \quad &G_i = 1, G_i' = 0 \text{ at } \zeta = 0 \\ &G_i = 0 \text{ at } \zeta = 1. \end{aligned} \quad (18)$$

Primes denote differentiation with respect to ζ. The C_i coefficients in equation (17) are determined from the condition $\theta = 1$ at $\chi = 0$. Since the eigenfunctions of equation (18) are orthogonal with respect to the weighting function $w(\zeta)$, where

$$w(\zeta) = f_j'(\zeta) \exp\left(Pe_W \int_0^{\zeta} \frac{f_j(z)}{z^j} \mathrm{d}z\right) \quad (19)$$

the C_i values are given by

$$C_i = \int_0^1 \theta(0, \zeta)\, w(\zeta)\, G_i(\zeta)\, \mathrm{d}\zeta \Big/ \int_0^1 w(\zeta)\, G_i^2(\zeta)\, \mathrm{d}\zeta \quad (20)$$

where, for the C.W.T. case, $\theta(0, \zeta) = 1$.

From the definition of the Nusselt number, and a relation obtained by integrating equation (18) from $\zeta = 0$ to 1, one obtains

$$Nu = \frac{\sum_{i=1}^{\infty} C_i(1 + (1 + j)Pe_W\chi)^{-\beta_i^2/Pe_W} G_i'(1)}{\sum_{i=1}^{\infty} \dfrac{C_i[1 + (1 + j)Pe_W\chi]^{-\beta_i^2/Pe_W}}{(\beta_i^2 - Pe_W)} G_i'(1)}. \quad (21)$$

For large values of χ, the first terms in the series will dominate. Therefore, the fully developed Nusselt number is

$$Nu_{fd} = \beta_1^2 - Pe_W. \quad (22)$$

Equation (22), for tube flow, was given previously by Kinney [3]. Note that the value of β_1^2, and thus Nu_{fd}, for tube flow will be different from that for duct flow. In fact, all of the constants β_i^2 and C_i and all the functions $G_i(\zeta)$ and $w(\zeta)$ will be different for the two geometries so that solutions must be carried out separately for $j = 0$ and $j = 1$.

The above results contain, as special cases, the solutions for no mass transfer across the wall. This may be seen immediately by recognizing that

$$\lim_{\{Pe_W \to 0\}} [1 + (1 + j)\, Pe_W\chi]^{-\beta_i^2/Pe_W} = \exp[-(1 + j)\beta_i^2\chi].$$

Numerical results are obtained by computing the functions $f_j(\zeta)$ and $f_j'(\zeta)$ from equations (3A)–(7) for tube flow ($j = 1$) or from equations (10)–(12) for duct flow ($j = 0$). Introducing these into equation (18) and specifying Pe_W permits $G_i(\zeta)$ and β_i^2 to be found numerically. The temperature profile and Nusselt number at any value of χ can be found respectively from equations (17) and (21); the fully developed Nusselt number can be found from equation (22) once the first eigenvalue is known. For each chosen Re_W and Pe_W, enough terms in the series were obtained to guarantee a Nu value accurate to about 0·5 per cent over the desired range of χ. Development lengths, defined as the distance χ_{fd} at which $Nu = 1{\cdot}05\, Nu_{fd}$, were determined for all cases. Values of C_i, $G_i'(1)$, etc. for both tube and duct flow, for the special case $Re_W = 0$, agreed with Brown's results [10] to 9 figures. Computed constants and coefficients are available on request.

C.W.T. results for tubes and ducts

(a) *Fully developed region.* Before presenting solutions (to) the above equations, it is instructive to examine certain limiting cases so that the influence of wall mass transfer on the fully

developed temperature profile, for example, can be physically understood. First consider the case $Pe_W \to \infty$.

A large positive wall Péclét number ($Re_W > 0$) implies that the convective heat transport away from the wall is large compared to the transport by conduction in the same direction. As $Pe_W \to \infty$, the wall becomes blanketed by a layer of fluid having a temperature very close to T_W, and therefore $Nu_{fd} \to 0$. Note that the Péclét number can be large if either (a) the blowing rate is high ($Re_W \to \infty$) but the Prandtl number is low or moderate or if (b) the Prandtl number is high, even though the blowing rate is small ($Re_W \to 0$). For $Pe \to \infty$, closed form asymptotic temperature profiles are obtained in Appendix A for both cases (a) and (b) and for both tube and duct geometries. In all cases, this profile is flat at the wall and near the centreline, $[(T - T_W)/(T_{\mathfrak{L}} - T_W)]_{fd} = \exp[-CPe_W\zeta^2]$ where C is a constant. The asymptotic results are compared below with the "exact" solutions.

For flow with suction, the influence of the cooled or heated wall will be restricted to a thermal layer near the wall. The thickness of this layer reflects the distance which heat conducted from the wall can penetrate into the fluid moving towards the wall. The higher the suction rate and/or the higher the Prandtl number, the thinner will be the thermal layer. That is, if Δ represents the thickness of the thermal layer, $\Delta \to 0$ as $Pe_W \to -\infty$. For small Δ, most of the fluid heated by conduction is immediately withdrawn through the wall so that very little heat is transferred to the central portion of the tube or duct. Therefore, $\partial T/\partial x \to 0$ and $[(T - T_W)/(T_{\mathfrak{L}} - T_W)]_{fd} \to 1$ as $Pe_W \to -\infty$ (see Appendix A).

Since, for this case, the heat transferred by conduction to the fluid $[\approx k(T_W - T_{\mathfrak{L}})/\Delta]$ is nearly equal in magnitude but opposite in direction to the heat convected from the fluid through the wall $[\approx \rho C_p v_W(T_W - T_{\mathfrak{L}})]$, one obtains from the definition of Pe_W, $Pe_W \approx -2R/\Delta$. For large negative Pe_W therefore, the wall Péclét number physically represents the ratio of the tube diameter to the thickness of the thermal layer.

The "exact" solutions for the fully developed temperature profile, the solid curves in Figs. 5 and 6, display the trends expected from the

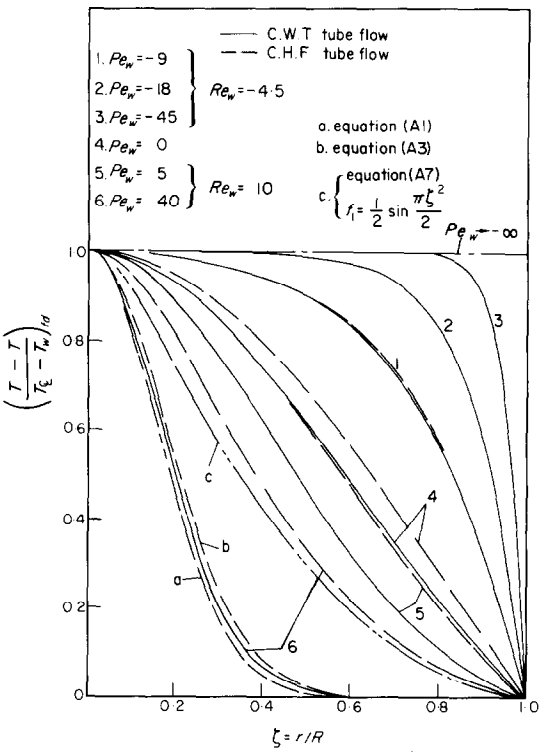

FIG. 5. Fully developed temperature profiles for flow in a circular tube with constant wall temperature and constant heat flux.

asymptotic solutions. For no mass transfer through the wall, $Re_W = 0$, the results are already well known. For suction, $Re_W < 0$, the profile becomes fuller with larger negative values of Pe_W, and $[(T - T_W)/(T_{\mathfrak{L}} - T_W)]_{fd}$ asymptotically approaches unity, as expected. For injection, $Re_W > 0$, the profile drops off more quickly to zero. The asymptotic solutions are compared to the computed values for $Pe_W = 40$ in Figs. 5 and 6 for $Re_W = 10$. For the same value of Pe_W, but for larger Re_W, the computed results would tend toward curve a, and for smaller Re_W toward curve b. The close-

ness of curves a and b illustrates that the fully developed profile is known quite precisely if only Pe_W is specified; the particular Re_W, Pr combination, whose product equals the numerical value of Pe_W, is relatively unimportant. A similar result will be shown with respect to the

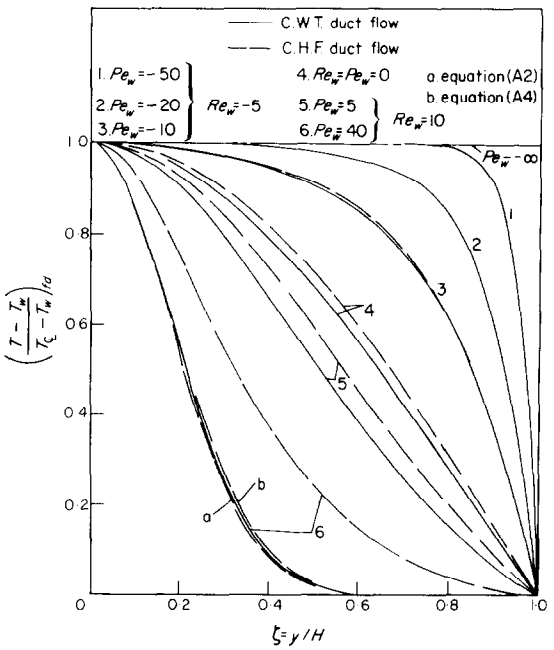

FIG. 6. Fully developed temperature profiles for two-dimensional rectangular duct flow with constant wall temperature and constant heat flux.

Nusselt number and development length computations. Therefore the advantage of choosing Re_W and Pe_W as parameters, rather than the usual Re_W and Pr, is considerable.

Nusselt numbers in the thermally developed regions of tubes and ducts are shown in Figs. 7 and 8 (solid curves) respectively. These were computed using equation (22). The general trends are those anticipated, namely $Nu_{fd} \to 0$ as $Pe_W \to \infty$, and as $Pe_W \to -\infty$, $Nu_{fd} \to -Pe_W$ (from equation (22) since, from Appendix A, $\beta_1^2 \to 0$ as $Pe_W \to -\infty$).

For tube flow with mass injection (Fig. 7), results are shown for the two extreme velocity profiles corresponding to $Re_W \to 0$ and $Re_W \to \infty$. Results for all intermediate blowing rates must fall between these extremes; computations for $Re_W = 5$ and 10 are shown. It will be noted that Nu_{fd} is also primarily a function of Pe_W, depending only weakly on Re_W. This is even more evident for duct flow, Fig. 8, where the curves corresponding to the extreme cases are almost identical.

For suction, computations for tube flow are reported for the two extremes $Re_W \to 0$ and $Re_W = -4{\cdot}5978$, the latter being near the critical value where the wall velocity gradient becomes zero. Other curves for $-4 < Re_W < 0$ were found to be grouped near the curve for $Re_W \to 0$; only for Re_W values close to the critical did the Nu_{fd} vs. Pe_W curve become sensitive to Re_W. For duct flow with suction, Fig. 8 shows that the results for $Re_W \to 0$ and $Re_W = -15$ are almost identical. Results corresponding to the slug flow case, $Re_W \to -\infty$, are also included but, from the previous discussion, the existence of laminar profiles for $-24 > Re_W > -\infty$ is open to question.

(b) *Thermal entrance region.* For the calculation of heat or mass transfer rates, it is important to know how the Nusselt number changes in the thermal entrance region and in what axial distance the development occurs.* Nusselt number distributions in the entrance regions are shown for tubes and ducts in Figs. 9 and 10 respectively. The similarity of the distributions for a large range of Re_W, but for a given Pe_W, is apparent, particularly for duct flow. The upper curves in Fig. 9 are terminated at the point $\chi = 0{\cdot}05$ where all the mass has been removed from the tube.

The dimensionless development lengths, i.e. the values of χ for which $Nu = 1{\cdot}05\ Nu_{fd}$, for tubes and ducts are shown in Fig. 11. The dominant features are (1) the strong increase in χ_{fd} with Pe_W, and (2) the nearly unique dependence of χ_{fd} on Pe_W except for values of Re_W near the critical value for the tube and for the slug flow case ($Re_W \to -\infty$) for the duct. As already pointed out, solutions for $Re_W < -24$

* Results of other computations, such as mean and centerline temperatures are available on request.

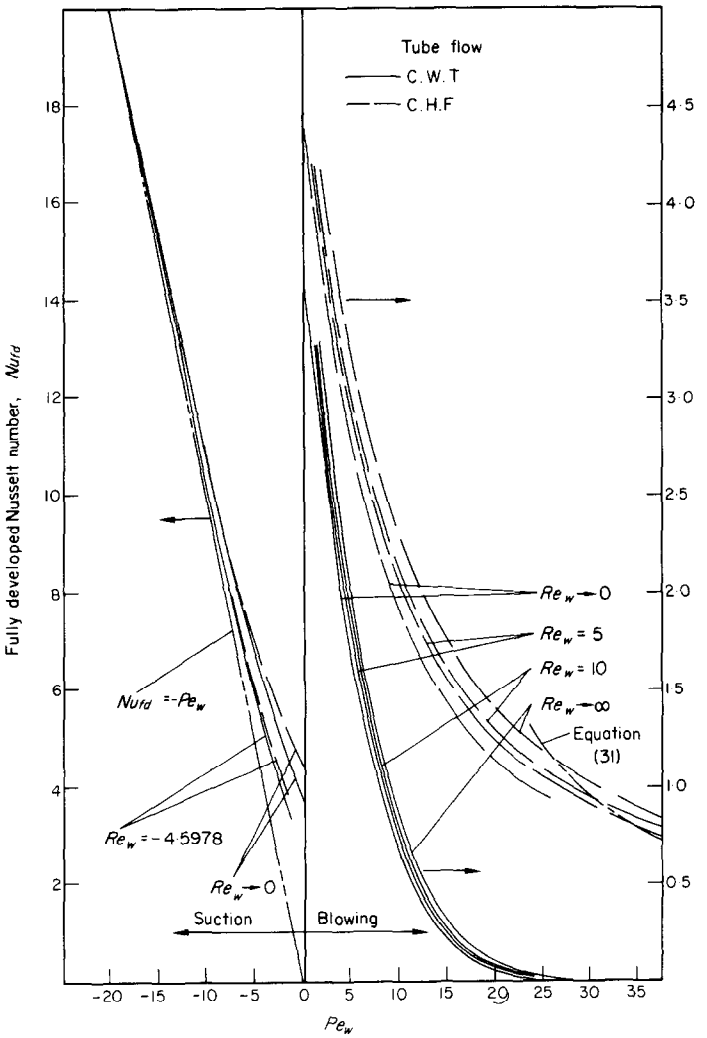

FIG. 7. Dependence of Nusselt number on Re_W in the thermally developed region of a circular tube.

for the duct flow may have no physical significance—thus the question mark near the upper curve in Fig. 11. In terms of the more familiar parameters of Pr and Re_W, Fig. 11 illustrates that, for a given Prandtl number, suction decreases the thermal development length and injection increases it.

C.H.F. solutions for tubes and ducts

The temperature field and Nusselt number distributions in the thermal entrance region with a constant heat flux boundary condition are now sought. It is assumed that the fluid and wall have a uniform temperature T_0 up to some point $x = 0$, where the velocity field is fully developed, and that for $x > 0$, q_W is constant. The method used here, analogous to that of Siegel *et al.* [11], involves first obtaining the fully developed temperature profile. The difference between the developing temperature

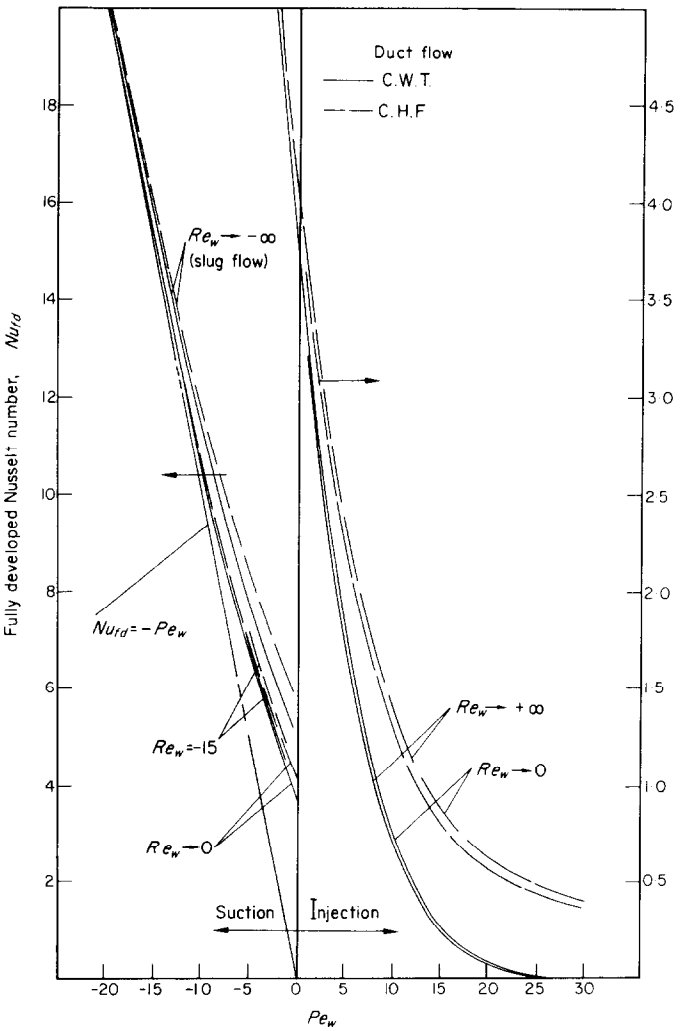

FIG. 8. Dependence of Nusselt number on Re_w in the thermally developed region of a two-dimensional rectangular duct.

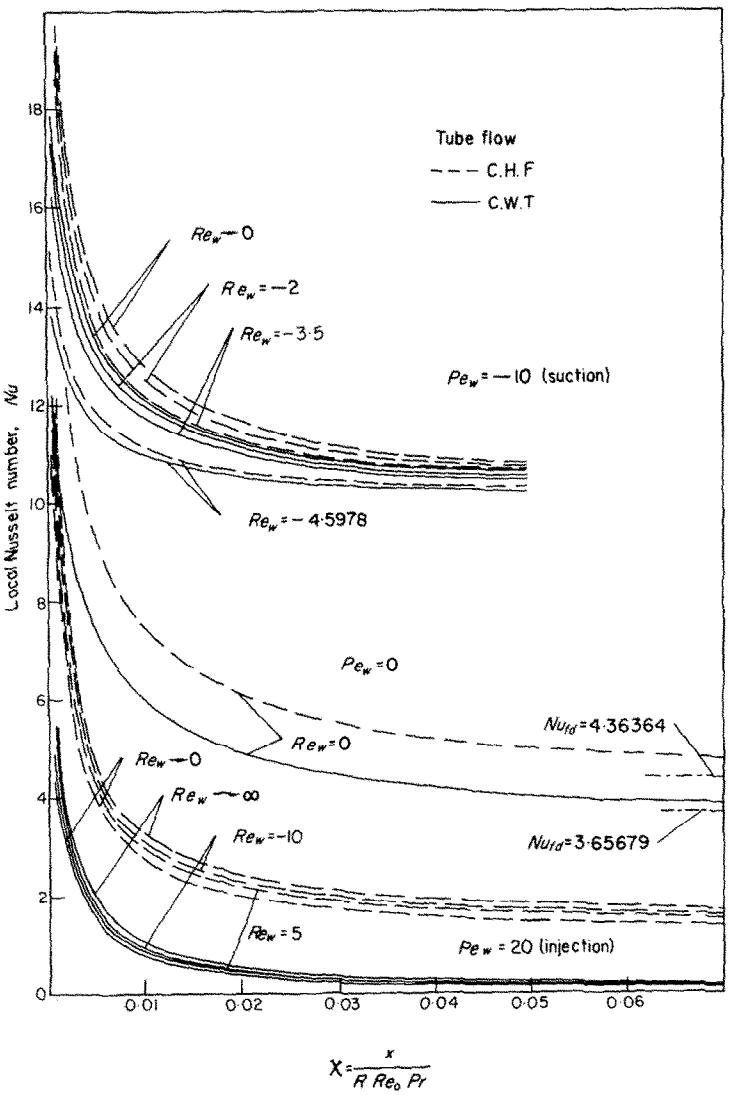

FIG. 9. Nusselt number distributions in the thermal entrance region of a circular tube.

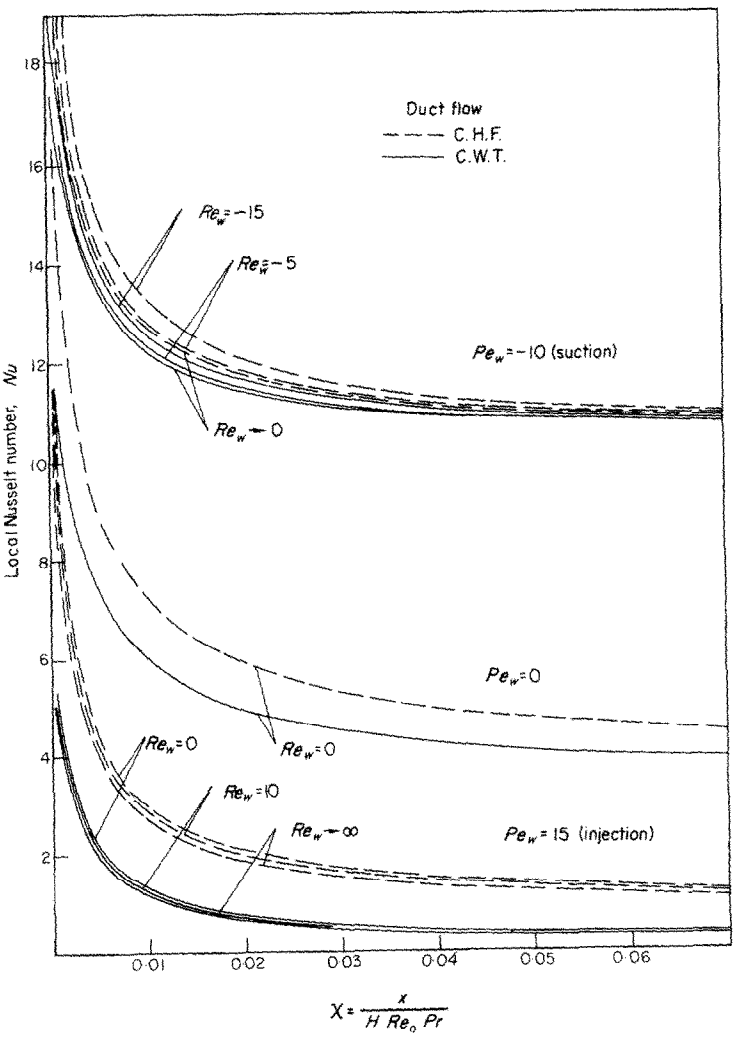

FIG. 10. Nusselt number distributions in the thermal entrance region of a two-dimensional rectangular duct.

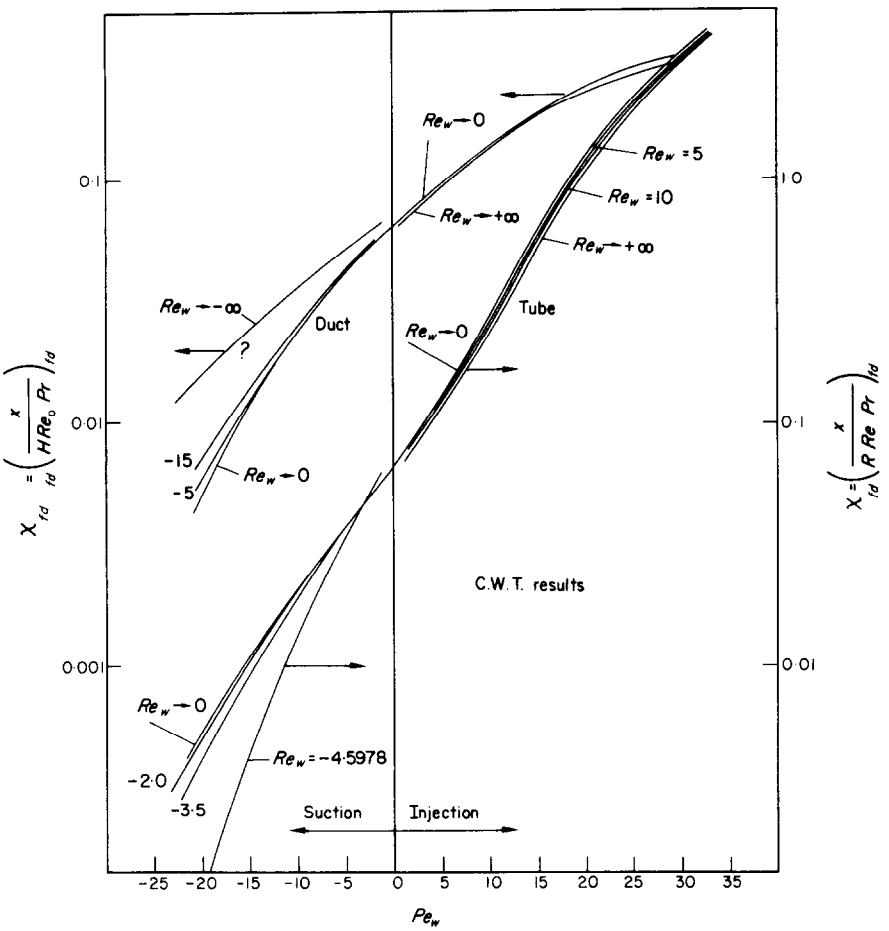

FIG. 11. Development lengths for flow in circular tubes and two-dimensional rectangular ducts with a constant wall temperature.

profile and the developed profile is then determined by applying the Graetz method.

Analysis for thermally developed region, C.H.F. case. For the C.H.F. case, the dimensionless temperature, θ is redefined as $\theta = k(T - T_0)/q_W R$ for the tube and $\theta = k(T - T_0)/q_W H$ for the duct. In the developed region, the shape of the temperature profile will be independent of x but the temperature level may still depend on the axial position. Accordingly, we seek a fully developed dimensionless temperature, θ_{fd}, having the form

$$\theta_{fd} = R(\chi) + h(\zeta). \tag{23}$$

By substituting this expression into equations (14) and (15) for the tube and duct respectively, and requiring that all the boundary conditions except $T = T_0$ at $x = 0$ be satisfied, one obtains the form of the function $R(\chi)$ and the governing equation for $h(\zeta)$. For either geometry,

$$\theta_{fd} = \frac{B_j}{(1+j)Pe_W} - \ln\left[1 + (1+j)\,Pe_W\chi\right] + h(\zeta) \tag{24}$$

where $j = 1$ for the tube and $j = 0$ for the duct.

For $h(\zeta) = g(\zeta) - K$ (K is some constant), $g(\zeta)$ is defined by the following equation; primes denote differentiation with respect to ζ

$$\zeta^j g'' + (j + Pe_W f_j)\,g' - \frac{B_j}{2} f_j' = 0$$

$$\text{b.c.} \qquad \zeta = 0: \quad g = 1, \quad g' = 0 \tag{25}$$

$$\zeta = 1: \quad g' = 1.$$

The three boundary conditions are sufficient to determine $g(\zeta)$ and B_j in equation (25). $g(0)$ may be assigned arbitrarily, the effect on $h(\zeta)$ being simply to change the value of K. From the definition of bulk temperature, the constant K is found to be

$$K = 2\int_0^1 f_j'(\zeta)\,g(\zeta)\,\mathrm{d}s. \tag{26}$$

The analysis for the thermally developed region is thus complete. This solution contains, as a special case, the solution for $Re_W = 0$. For tube flow with $Re_W = 0$, $f_1 = \zeta^2 - \zeta^4/2$, so that equation (25) can be immediately integrated. To obtain the result derived by Siegel *et al.* [11] requires only the additional observation that

$$\lim_{Pe_W \to 0}\left(\frac{B_1}{2Pe_W}\ln(1 + 2Pe_W\chi)\right) = B_1\chi$$

where $B_1 = 4$.

Results for the fully developed region. The dimensionless temperature profile in the full developed region is, from equation (23),

$$\left[(T - T_W)/(T_{\mathfrak{L}} - T_W)\right]_{fd} = \left[g(\zeta) - g(1)\right]/\left[g(0) - g(1)\right]. \tag{27}$$

An understanding of the effect of blowing and suction on the temperature profile may be obtained by considering asymptotic solutions to equation (25) for large values of Pe_W. The results, given in Appendix A, indicate that the dimensionless temperature does not decrease near the centreline nearly as rapidly for increasing positive values of Pe_W as in the C.W.T. case. For $Pe_W \to -\infty$ however, the same asymptotic temperature profile is obtained for either the C.W.T. or C.H.F. case, namely $\left[T - T_W\right)/(T_{\mathfrak{L}} - T_W)\right]_{fd} \to 1$.

Dimensionless temperature profiles were obtained by solving equation (25) numerically for the same Re_W and Pe_W values as in the C.W.T. case. These results, the asymptotic solutions and the C.W.T. results for tube flow are all plotted together in Fig. 5. For large negative Pe_W, the profiles become flatter, as expected, and the C.W.T. and C.H.F. profiles become indistinguishable (curves 2 and 3). The C.H.F. asymptotic solution for $Pe_W = 40$ (equation (A7) with $f_1 = \frac{1}{2}\sin\pi\zeta^2/2$) predicts the correct profile shape; the quantitative agreement between the asymptotic solution and the exact solution becomes substantially improved for larger Re_W and Pe_W values. Also, the differences between the C.W.T. and C.H.F. profiles become more pronounced for large positive Pe_W. Figure

6 shows the corresponding results for the duct flow case.

The expression for the fully developed Nusselt number is found from equation (24) to be

$$Nu_{fd} = \frac{2}{h(1)} = \frac{Pe_W}{[B_j/2(j+1)] - 1}. \quad (28)$$

The second equality comes from integrating equation (25) from $\zeta = 0$ to $\zeta = 1$. $h(1)$ and B_j, and therefore Nu_{fd}, can be found by solving equation (25) numerically. Another method is to integrate equation (25) over the cross-section and use the boundary condition $g'(1) = 1$ to obtain the equation

$$B_j = 2\exp\left(Pe_W \int_0^1 \frac{f_j(z)}{z^j}\,dz\right) \Big/ \int_0^1 f_j'(\zeta)\exp\left(Pe_W \int_0^\zeta \frac{f_j(x)}{z^j}\,dz\right)d\zeta. \quad (29)$$

Once the velocity profile (f_0 for duct or f_1 for tube) is known for the required value of Re_W, equation (29) can be integrated numerically for the desired Pe_W to obtain B_j.

It is shown in Appendix A that, for large negative values of Pe_W, $B_j \to 0$ so that, from equation (28), $Nu_{fd} \to -Pe_W$ as $Pe_W \to -\infty$. This is the same result as for the C.W.T. case. Also from the Appendix, we could expect that $Nu_{fd} \to 0$ as $Pe_W \to \infty$. To determine how rapidly the Nusselt number decreases with increasing Pe_W, consider flow in a tube with a low blowing rate ($Re_W \to 0$) where $f_1 \approx \zeta^2 - \zeta^4/4$. If the Prandtl number is very large, Pe_W would also be large so that an approximate solution to equation (29) is

$$B_1 \to Pe_W \Big/ \left(\frac{2^3}{Pe_W} - \frac{3.2^5}{Pe_W^2} + \frac{5.3.2^7}{Pe_W^3}\right). \quad \text{(tube)} \quad (30)$$

From equation (28),

$$Nu_{fd} \to \frac{32\alpha}{Pe_W}\left[1 - \frac{32\alpha}{Pe_W}\right];$$

$$\alpha = 1 - \frac{12}{Pe_W} + \frac{240}{Pe_W^2} \quad \text{(tube)} \quad (31)$$

$$\approx 32/Pe_W \text{ for } Pe_W \to \infty \text{ but } Re_W \to 0.$$

For the same geometry, but for large blowing rates and moderate or small Prandtl number, it would be expected that Nu_{fd} would be still given approximately by the same equation. A similar solution could presumably be found for duct flow.

The B_j values found by numerically integrating equation (25) were introduced into equation (28) to give values of Nu_{fd}. The results for tube flow ($j = 1$) are shown by the dashed curves in Fig. 7. The C.W.T. results are also shown for comparison. The expected trends are indicated, namely $Nu_{fd} \to -Pe_W$ for $Pe_W \to -\infty$, and for $Pe_W \to \infty$ but Re_W small, equation (31) is asymptotically approached. The corresponding results for duct flow ($j = 0$) are shown in Fig. 8.

Analysis and results for thermal entrance region, C.H.F. case. Following the method of Siegel *et al.* [11] for flow without mass transfer, a temperature θ^* is defined by

$$\theta^* = \theta - \theta_{fd} \quad (32)$$

where θ is the temperature profile in the developing region and θ_{fd} is the fully developed profile found in the previous section. Substituting θ into equation (16) and applying the boundary conditions, it follows that θ^* is described by the problem

$$\frac{1}{f_j'}\frac{\partial}{\partial\zeta}\left(\zeta^j\frac{\partial\theta^*}{\partial\zeta}\right) + \frac{f_j}{f_j'}Pe_W\frac{\partial\theta^*}{\partial\zeta} = \frac{1}{(j+1)}\frac{\bar{u}(\chi)}{\bar{u}_0}\frac{\partial\theta^*}{\partial\chi} \quad (33)$$

$$\zeta = 0: \quad \frac{\partial\theta^*}{\partial\zeta} = 0; \qquad \zeta = 1: \quad \frac{\partial\theta^*}{\partial\zeta} = 0;$$

$$\chi = 0: \quad \theta^* = -\theta_{fd}.$$

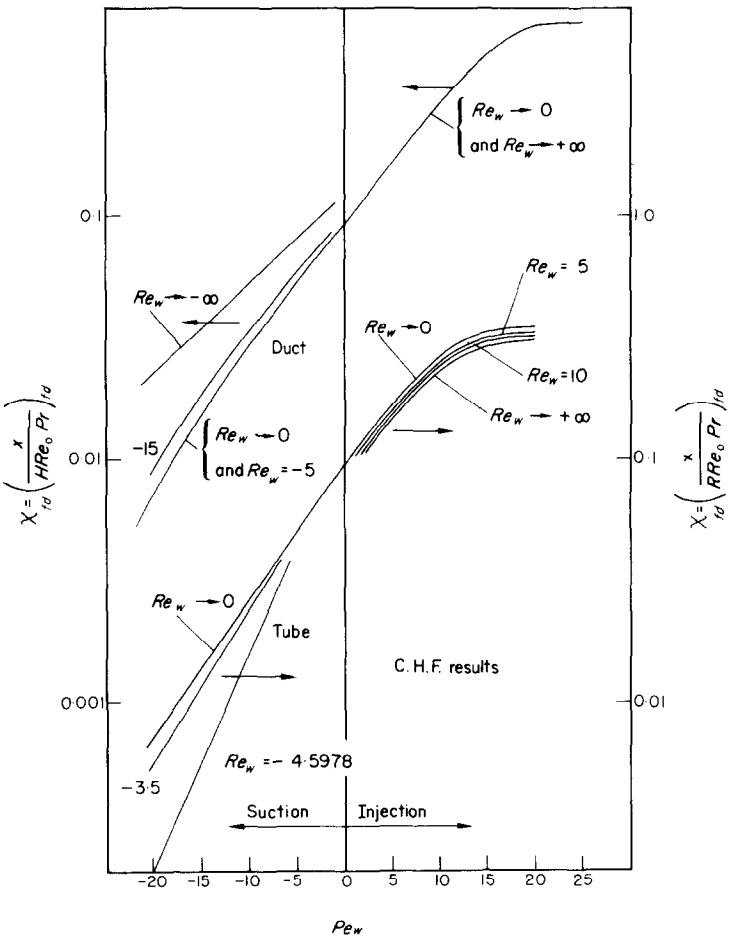

FIG. 12. Development lengths for flow in circular tubes and two-dimensional rectangular ducts with constant heat flux at the wall.

Solutions for θ^* are found by a method (Graetz method) exactly analogous to the solutions for θ in the C.W.T. problem. In this case

$$\theta^* = \sum_{i=1}^{\infty} C_i[1 + (1 + j)\, Pe_W\chi]^{-\beta_i^2/Pe_W}\, G_i(\zeta). \tag{34}$$

G_i is described by equation (18) with $G_i'(1) = 0$ replacing the boundary condition $G_i(1) = 0$. The weighting function remains unchanged. The analysis for θ^* is thus complete.

From equation (32), and the equations for θ_{fd}, the desired solution for θ is

$$\theta = \frac{B_j}{(1 + j)Pe_W} \ln[1 + (1 + j)Pe_W\chi] + h(\zeta) + \sum_{i=1}^{\infty} C_i(1 + (1 + j)Pe_\chi\chi)^{-\beta_i^2/Pe_W} G_i(\zeta). \tag{35}$$

Using the definition of the bulk temperature and the result of integrating equation (33) from 0 to 1, it follows that the local Nusselt number in the thermal entrance region is

$$Nu = \frac{2/h(1)}{1 + \sum_{i=1}^{\infty} \frac{C_i G_i(1)}{h(1)} \left(\frac{\beta_i^2}{\beta_i^2 - Pe_W}\right)[1 + (1 + j)Pe_W\chi]^{-\beta_i^2/Pe_W}}.$$

Entrance region Nusselt numbers for tube flow are shown in Fig. 9 (dashed curves) for $Pe_W = -10$, 0 and 20. Although the curves for the injection case for C.H.F. lie considerably above their C.W.T. counterparts, the trends are similar in all cases. Similar results for duct flow are shown in Fig. 10.

The dependence of entrance length on Pe_W and Re_W for tube and duct flow with a C.H.F. boundary condition is shown in Fig. 12. Again the trends are similar to those in Fig. 11 for the C.W.T. case. In view of the previous discussion, it is not known if the slug flow case ($Pe_W \to -\infty$) has physical significance.

Arbitrary wall-temperature and heat-flux variations. Since the energy equation is linear, the superposition principle can be used to extend the above calculations to cases where the wall temperature or heat flux varies in an arbitrary manner. The method is completely analogous to that described by Sellars *et al.* [12] for the C.W.T. case, and Siegel *et al.* [11] for the C.H.F. case. Because this procedure is so widely known, no further enumeration is necessary.

ACKNOWLEDGEMENTS

The author wishes to thank the National Research Council of Canada for financial support, Mr. B. McDonald for assistance in programming the velocity problems, several colleagues at the University of Waterloo for helpful discussions, and Mrs. R. Trenberth for typing the manuscript.

REFERENCES

1. E. R. G. Eckert, P. L. Donoughe and B. L. Moore, Velocity and friction characteristics of laminar viscous boundary-layer and channel flow over surfaces with ejection or suction, NACA TN4102 (1957).
2. A. S. Berman, Effects of porous boundaries on the flow of fluids in systems with various boundaries, *Proc. Second United Nations International Conference on the Peaceful Uses of Atomic Energy, Geneva* **4**, 351–358 (1958).
3. R. B. Kinney, Fully developed frictional and heat-transfer characteristics of laminar flow in porous tubes, *Int. J. Heat Mass Transfer* **11**, 1393–1401 (1968).
4. S. W. Yuan and A. B. Finkelstein, Heat transfer in laminar pipe flow with uniform coolant injection, *Jet Propulsion* **28**, 178–181 (1958).
5. S. W. Yuan and A. B. Finkelstein, Laminar pipe flow with injection and suction through porous walls, *Trans. Am. Soc. Mech. Engrs* **78**, 719–724 (1956).
6. B. Thwaites, *Incompressible Aerodynamics*, pp. 28–290. Clarendon Press, Oxford (1960).
7. A. S. Berman, Laminar flow in channels with porous walls, *J. Appl. Phys.* **24**, 1232–1235 (1953).
8. S. W. Yuan, Further investigations of laminar flow in channels with porous walls, *J. Appl. Phys.* **27**, 267 (1956).
9. R. J. Pederson, Entry region heat transfer characteris-

tics for laminar flow in porous tubes, Master of Science Thesis, Aerospace and Mechanical Engineering Dept., University of Arizona (1969).
10. G. M. BROWN, Heat or Mass transfer in laminar flow in a circular or flat conduit, *A.I.Ch.E. Jl* **6**, 179–183 (1960).
11. R. SIEGEL, E. M. SPARROW and T. M. HALLMAN, Steady laminar heat transfer in a circular tube with prescribed wall heat flux, *Appl. Sci. Res.* **7A**, 386–392 (1958).
12. J. R. SELLARS, M. TRIBUS and J. S. KLEIN, Heat transfer in a round tube or flat conduit—The Graetz problem extended, *Trans. Am. Soc. Mech. Engrs.* **78**, 441–448 (1956).
13. E. R. G. ECKERT and R. M. DRAKE, *Heat and Mass Transfer*. McGraw-Hill, New York (1959).

APPENDIX A

In the text, physical reasoning lead to conclusions, for asymptotically large negative and positive Pe_W, which can be used to derive asymptotic temperature profiles. These solutions for C.W.T. and C.H.F. will be considered in turn.

(a) *C.W.T.*, $\mathrm{Pe_W} \to \infty$

In the section, "C.W.T. Results for Tubes and Ducts", it was reasoned that, $Nu_{fd} \to 0$ as $Pe_W \to \infty$. From equation (22), therefore, $\beta_1^2 \to Pe_W$ as $Pe_W \to \infty$. Introducing this into equation (18) results in

$$(\xi^j G_1')' + Pe_W(f_j G_1)' = 0.$$

This equation can be integrated for either the tube geometry ($j = 1$) or duct geometry ($j = 0$) if the velocity profile, i.e. f_j, is known. The velocity profiles for the limiting cases of small and large injection rates are indicated in Table 1. Introducing these into the above equation, direct integration and application of boundary conditions at $\zeta = 0$ leads to solutions of $G_1(\zeta)$ for $Pe_W \to \infty$. This gives the developed temperature profile for large Pe_W since, from equation (17)

$$G_1(\zeta) = [(T - T_W)/(T_{\mathbb{Q}} - T_W)]_{fd}.$$

The solutions are listed in Table 1, equations (A1)–(A4).

(b) *C.W.T.*, $\mathrm{Pe_W} \to -\infty$

For this condition, it is shown in the text that there is little heat transfer into the central portion of the tube or duct. In terms of the axial temperature gradient, $\partial T/\partial x \to 0$ as $Pe_W \to -\infty$. Since $\beta_1^2 = (\bar{u}/2\bar{u}_0)\,\partial\theta/\partial\chi$, $\beta_1^2 \to 0$ as $Pe_W \to -\infty$. Integrating equation (18) leads to $G_1(\xi) \to 1$ for $j = 0$ or $j = 1$ and for any velocity profile. That is, $[T - T_W)/(T_{\mathbb{Q}} - T_W)]_{fd} \to 1$ as $Pe_W \to -\infty$. This result is also listed in Table 1.

(c) *C.H.F.*, $\mathrm{Pe_W} \to \infty$, *tube flow*

From equation (24), for C.H.F.,

$$[(T - T_W)/(T_{\mathbb{Q}} - T_W)]_{fd} = [g(\zeta) - g(1)]/[g(0) - g(1)] \quad \text{(A6)}$$

where $g(\zeta)$ is the solution to equation (25). To find a first approximation to the solution for tube flow for $Pe_W \to \infty$, the $\zeta g''$ term in equation (25) can be neglected compared to the other terms. This reduces the order of the differential equation and, as a result, the boundary condition $g'(1) = 1$ can not be satisfied. Direct integration leads to the result.

$$[T - T_W)/(T_{\mathbb{Q}} - T_W)] \simeq 1 - \ln(1 + Pe_W f_1)/(\ln(1 + Pe_W/2)) \quad \text{(A7)}$$

Table 1. Asymptotic fully developed temperature profiles, C.W.T. case

Geometry	Re_W	Pe_W	Asymptotic velocity profile, $u/\bar{u}$	Asymptotic temperature profile $[(T - T_W)/(T - T_W)]_{fd}$	Equation
tube	$\to \infty$	$\to \infty$	$\to \pi/2 \cos(\pi\zeta^2/2)$	$\to \exp\left[-\frac{Pe_W}{4}\left(\frac{\pi\zeta^2}{2} - \frac{(\pi\zeta^2/2)^3}{3\cdot 3!} + \ldots\right)\right]$	(A1)
duct	$\to \infty$	$\to \infty$	$\to \pi/2 \cos(\pi\zeta/2)$	$\to \exp\left[-\frac{Pe_W}{\pi}\left(1 - \cos\frac{\pi\zeta}{2}\right)\right]$	(A2)
tube	$\to 0$	$\to \infty$	$\to 2(1 - \zeta^2)$	$\to \exp\left[-\frac{Pe_W}{2}\zeta^2\left(1 - \frac{\zeta^2}{4}\right)\right]$	(A3)
duct	$\to 0$	$\to \infty$	$\to (3/2)(1 - \zeta^2)$	$\to \exp\left[-\frac{3Pe_W}{8}\left(\zeta^2 - \frac{\zeta^4}{6}\right)\right]$	(A4)
tube or duct	—	$\to -\infty$	—	$\to 1$	(A5)

for $Pe_W \to \infty$. This indicates that, for the C.H.F. case, the temperature does not decrease as rapidly with Pe_W near the centerline as in the C.W.T. case. Either of the asymptotic velocity profiles for $Re \to 0$ and $Re_W \to \infty$ can be introduced into equation (A7).

(d) *C.H.F.*, $Pe_W \to -\infty$

By the same reasoning as in the C.W.T. case, $\partial T/\partial x \to 0$ as $Pe_W \to \infty$. Since $B_j = [\bar{u}(\chi)/\bar{u}_0]\partial\theta_j/\partial\chi$, $B_j \to 0$ as $Pe_W \to -\infty$. For this limiting case, for any velocity profile, equation (25) yields the result $g(\xi) \to g(0)$ so that from equation (A6)

$$[(T - T_W)/(T_\mathbb{C} - T_W)]_{fd} \to 1 \text{ as } Pe_W \to -\infty. \quad \text{(A8)}$$

TRANSFERT DE CHALEUR LAMINAIRE DANS LA RÉGION D'ENTRÉE THERMIQUE DE TUBES CIRCULAIRES ET DE CONDUITS RECTANGULAIRES BIDIMENSIONNELS AVEC SUCTION ET INJECTION PARIÉTALES

Résumé—Des profils développés de vitesse, pour des écoulements avec addition ou soustraction de masse aux frontières, sont établis pour les géométries correspondant à la fois à un tube circulaire et à un conduit rectangulaire bidimensionnel. Pour un écoulement dans un conduit bidimensionnel on a trouvé une nouvelle solution qui suppose la possibilité d'une transition vers la turbulence induite par suction. Des équations représentant les coefficients de frottement sont présentées pour les deux géométries. Le développement du champ de température dans une région de vitesse entièrement développée est analysé pour les deux conduits et pour des conditions aux limites de température constante et de flux thermique constant. On démontre la dépendance presque universelle des résultats du transfert thermique à un unique paramètre, un nombre de Péclet basé sur la vitesse du fluide traversant la paroi. Plusieurs solutions asymptotiques relatives à l'équation d'énergie sont obtenues pour des hauts flux massiques d'addition et soustraction.

LAMINARE WÄRMEÜBERTRAGUNG IM THERMISCHEN EINLAUFGEBIET KREISFÖRMIGER ROHRE UND ZWEIDIMENSIONALER RECHTECKKANÄLE MIT ABSAUGEN UND EINBLASEN AN DER WAND

Zusammenfassung—Es wird über ausgebildete Geschwindigkeitsprofile sowohl für kreisförmige Rohre als auch für rechteckige Kanalgeometrien bei Strömungen mit Massenzu- und abfuhr in der Grenzschicht bereichtet. Für die Strömung in einem zweidimensionalen Kanal wurde eine neue Lösung gefunden, die die Möglichkeit eines durch Absaugung hervorgerufenen Umschlages in Turbulenz andeutet. Gleichungen für die Reibungsbeiwerte werden für beide Geometrien angegeben. Die Entwicklung des Temperaturfeldes im Gebiet ausgebildeter turbulenter Strömung wird für beide Kanäle bei konstanter Temperatur und konstantem Wämestrom untersucht. Die nahezu universelle Abhängigkeit des Wärmeübergangs von einem einzigen Parameter, nämlich einer auf der Geschwindigkeit der durch die Wand tretenden Flüssigkeit basierenden Peclet-Zahl, wird gezeigt. Für grosse Massenzu- und abfuhr werden mehrere asymptotische Lösungen der Energiegleichung erhalten.

ЛАМИНАРНЫЙ ТЕПЛООБМЕН В НАГРЕТОЙ ВХОДНОЙ ОБЛАСТИ КРУГЛЫХ ТРУБ И ДВУМЕРНЫХ ПРЯМОУГОЛЬНЫХ ТРУБ ПРИ ОТСОСЕ И ИНЖЕКЦИИ НА СТЕНКЕ

Аннотация—В статье приводятся полностью развитые профили скорости для потоков с подачей или отводом массы через границу как для кольцевой трубы, так и двумерных прямоугольных геометрий трубопроводов. При течении в двумерном трубопроводе найдено новое решение, предлагающее возможность перехода к турбулентности, вызванной всасыванием. Уравнения, содержащие коэффициенты трения, представлены для обеих геометрий. Развитие температурного поля в области полностью развитой скорости анализируется как для трубопроводов, так и для граничных условий постоянной температуры и постоянной плотности теплового потока. Показана почти универсальная зависимость результатов переноса тепла от единого параметра, а именно числа Пекле, отнесенного к скорости жидкости, пересекающей стенку. Получено несколько асимптотических решений уравнения энергии для больших скоростей подачи и отбора массы.